

Visual axial PSF of diffractive trifocal lenses

Pedro J. Valle, José E. Oti, Vidal F. Canales, and Manuel P. Cagigal

Departamento de Física Aplicada Universidad de Cantabria.
Los Castros S/N, 39005. Santander, Spain.
vallep@unican.es

<http://www.optica.unican.es/>

Abstract: The ophthalmic applications of a diffractive trifocal lens design with adjustable add powers and light distribution in the foci are investigated. Axial PSFs of the trifocal lenses are calculated and analyzed as a function of the design parameters and the eye pupil size. The optical performance in actual eyes is also simulated by including the measured ocular wave aberration functions of human eyes in the calculation of transverse and axial PSFs, and Strehl ratio axial variation. The effect of the polychromatic character of natural light has also been considered. The calculus and simulation method of this paper can be applied for the design and analysis of any other kind of diffractive or refractive multifocal contact or intraocular lens.

©2005 Optical Society of America

OCIS codes: (330) Vision and Color, (330.7310) Vision, (330.4460) Ophthalmic optics.

References and links

1. A. L. Cohen, "Practical design of a bifocal hologram contact lens or intraocular lens," *Appl. Opt.* **31**, 3750-3754 (1992).
2. A. L. Cohen, "Diffractive bifocal lens designs," *Optom. Vis. Sci.* **70**, 461-468 (1993).
3. S. A. Klein, "Understanding the diffractive bifocal contact lens," *Optom. Vis. Sci.* **70**, 439-460 (1993).
4. G. M. Morris and L. T. Nordan, "Phakic intraocular lenses," *Opt. Photon News*, **15** n° 9, 26-31 (2004).
<http://www.osa-opn.org/abstract.cfm?URI=OPN-15-9-26>.
5. N. Chateau and D. Baude, "Simulated *in situ* optical performance of bifocal contact lenses," *Optom. Vis. Sci.* **74**, 532-539 (1997).
6. M. Larsson, C. Beckman, A. Nyström, S. Hård, and J. Sjöstrand, "Optical properties of diffractive, bifocal, intraocular lenses," *Appl. Opt.* **31**, 2377-84 (1992).
7. M. J. Simpson, "Diffractive multifocal intraocular lens image quality," *Appl. Opt.* **31**, 3621-3626 (1992).
8. D. A. Atchison and L. N. Thibos, "Diffractive properties of the Diffrax bifocal contact lens," *Ophthalmic Physiol. Opt.* **13**, 186-188 (1993).
9. S. Pieh, P. Marvan, B. Lackner, G. Hanselmayer, G. Schmidinger, R. Leitgeb, M. Sticker, C. K. Hitznerberger, A. F. Fercher, and C. Skorpik, "Quantitative performance of bifocal and multifocal intraocular lenses in a model eye: point spread function in multifocal intraocular lenses," *Arch. Ophthalmol.* **120**, 23-28 (2002).
10. J. L. Alió, M. Tovalato, F. de la Hoz, P. Claramonte, J.-L. Rodríguez-Prats, and A. Galal, "Near vision restoration with refractive lens exchange and pseudoaccommodating and multifocal refractive and diffractive intraocular lenses," *J. Cataract Refract. Surg.* **30**, 2494-2503 (2004).
11. M. Golub and I. Grossinger, "Diffractive optical elements for biomedical applications." <http://www.holoor.co.il/data/ready2/publications/Biospape.pdf>.
12. *Basics and Clinical Science Course Section 3: Optics, Refraction, and Contact Lenses*, (American Academy of Ophthalmology, San Francisco, 2002).
13. M. W. Farn and W. B. Veldkamp, "Binary Optics" in *Handbook of Optics Vol. II*, M. Bass, ed. (McGraw-Hill, New York, 1995), pp. 8.1-8.19.
14. M. Born and E. Wolf, *Principles of Optics* (University Press, Cambridge, UK, 1999).
15. L. N. Thibos, R. A. Applegate, J. T. Schweigerling, R. Webb, and VSIA Standards Taskforce members, *Standards for Reporting the Optical Aberration of Eyes*, Vol 35 of OSA Topics in Optics and Photonics Series (Optical Society of America, Washington, D.C., 2000), pp.232-244.
16. J. A. Martin and A. Roorda, "Predicting and assessing visual performance with multizone bifocal contact lenses," *Optom. Vis. Sci.* **80**, 812-819 (2003).

17. M. P. Cagigal, V. F. Canales, J. F. Castejón-Mochón, P. M. Prieto, N. López-Gil, and P. Artal, "Statistical description of wave-front aberration in the human eye," *Opt. Lett.* **27**, 37-39 (2002).
18. L. N. Thibos, X. Hong, A. Bradley, and R. A. Applegate, "Accuracy and precision of objective refraction from wavefront aberrations," *J. Vis.* **4**, 329-351 (2004). <http://journalofvision.org/4/4/9/>.
19. J. D. Marsack, L. N. Thibos, and R. A. Applegate, "Metrics of optical quality derived from wave aberrations predict visual performance," *J. Vis.* **4**, 322-328 (2004). <http://journalofvision.org/4/4/8/>.
20. R. Navarro, M. Ferro, P. Artal, and I. Miranda, "Modulation transfer functions of eye implanted with intraocular lens," *Appl. Opt.* **32**, 6359-6367 (1993).
21. L. N. Thibos, Y. Ming, X. Zhang, and A. Bradley, "The chromatic eye: a new reduced-eye model of ocular chromatic aberration in humans," *Appl. Opt.* **31**, 3594-3600 (1992).

1. Introduction

Ophthalmic applications of diffractive multifocal lenses have become of increasing interest during the last fifteen years. The two principal applications of multifocal lenses in Ophthalmology are the contact lenses for correcting presbyopia and the intraocular lenses implanted during cataract surgery to replace the crystalline lens [1-3]. In the first case, the reduction with age of the accommodation capability of the human eye (presbyopia) can be partially compensated with a bifocal contact lens. Bifocal lenses provide two optical powers to divide the incident light between two axially separated images. One optical power is used to clear distant vision and the other one is used for clear near vision. Similarly, in the second case, the natural accommodation lost with crystalline lens extraction (cataract surgery) is substituted by the two powers of the bifocal intraocular lens for distant and near vision. Another application, under investigation nowadays, is the phakic intraocular lens (essentially an implantable contact lens designed to work in conjunction with the patient's cornea and natural crystalline lens) as an alternative to LASIK or PRK for correcting ametropia and presbyopia [4].

A number of diffractive bifocal designs has been proposed by several manufacturers (3M, Pilkington Barnes-Hind, Pharmacia, AcriTec, Holo-Or) as alternative to refractive bifocal lenses, and studies of visual performance for these lenses have been carried out [5-11]. Diffractive lenses use a nearly periodic modulation of the lens surface to diffract light into several directions to focus light into several points simultaneously. Some benefits of diffractive, unlike refractive, multifocal lenses are less sensitivity to the pupil size (equivalently to the illumination level) and to lens displacement (decentration). A drawback might be the chromatic aberration of the diffractive structure, although this can be partially balanced with the dispersion of the lens material and also with the natural chromatic aberration of the eye [3, 6, 8]. Furthermore, the incorporation of a second diffractive profile may be useful to provide a degree of control over the chromatic aberration [1, 2].

Bifocal lens may not fully satisfy all the visual needs for a patient with limited or zero accommodation [12]. Even when the near and distant ranges are corrected appropriately, vision will not be clear in the intermediate range (approximately at the arm's length). For example, a patient with 1D (one diopter) of available accommodation wearing a standard bifocal lens with 2D add power will have a blurred zone between 50 and 100 cm. This problem may be solved with a trifocal lens with 1D and 2D add powers. Grating multiplexers consisting of diffractive phase profiles of the form $\arctan(b\cos(2\pi ax))$ or $b\cos(2\pi ax)$ have been used to split one beam into three beams with equal or different intensities. These grating designs can be directly extended to trifocal lenses by replacing the x coordinate by the squared of radial coordinate, r^2 [3, 13]. These continuous and smooth profiles have some additional advantages over standard sawtooth or stepped designs (like those of references 5 to 10). First, there are not acutely angled echelettes so a contact lens with this design should be more comfortable on the eye. Second, the open regions are wider than the corresponding open regions of the stepped lens and they will trap less volume of lachrymal (contact lens case) or aqueous fluid (intraocular lens case) within the grooves of the profile where debris accumulation can take place.

The aim of this paper is to study the ocular behavior of diffractive trifocal lenses with a phase profile of the form $b\cos(2\pi ar^2)$, where r is the radial coordinate and, a and b are design parameters. The analysis of the visual system performance is often made by means of the transverse point spread function (PSF) or the modulation transfer function. In the case of multifocal lenses the axial behavior of the eye should also be considered. In Section 2, we outline the method used to calculate the axial intensity (axial PSF) of the lenses by taking into account the actual eye aberration. The trifocal lens optical features are derived in Section 3, as well as their dependence on the design parameters and the pupil size. Special attention is paid to the control of the add optical powers and the relative intensity of every focus. In Section 4, we investigate the optical performance of the diffractive trifocal lens when combined with the natural ocular aberrations. This is done by calculating the transverse PSF and Strehl ratio axial variation of actual eyes from previous experimental data of the ocular wave aberration functions measured with a Hartmann-Shack wavefront sensor. Finally, in Section 5, we have briefly considered the effect of the polychromatic character of natural light in the performance of the diffractive lens.

2. Axial PSF calculation

The PSF is calculated as the squared modulus of the optical field amplitude in the focal region. Within the framework of the scalar diffraction theory, this amplitude can be written as [14],

$$A(v, \varphi, u) = A_0 \frac{1}{2\pi} \int_0^{2\pi} \int_0^1 P(\rho, \theta) \exp\left[-ik\left(v\rho \cos(\theta - \varphi) + \frac{1}{2}u\rho^2\right)\right] 2\rho d\rho d\theta, \quad (1)$$

where $v=(R/f)r$ and $u=(R/f)^2z$ are the radial and axial optical coordinates, respectively. r , φ , and z are the usual cylindrical coordinates with origin at the geometrical focus (see Fig. 1). R and f are the pupil radius and focal length of the eye, respectively. $\rho=r/R$ and θ are the polar coordinates in the exit pupil plane, $k=(2\pi)/\lambda$, and λ is the light wavelength. $P(\rho, \theta)$ is the complex pupil function of the optical system.

For the axial amplitude we set $v=0$, and then Eq. (1) becomes,

$$A(u) = A_0 \frac{1}{2\pi} \int_0^{2\pi} \left\{ \int_0^1 P(\rho, \theta) d\theta \right\} \exp\left[-ik\frac{1}{2}u\rho^2\right] 2\rho d\rho. \quad (2)$$

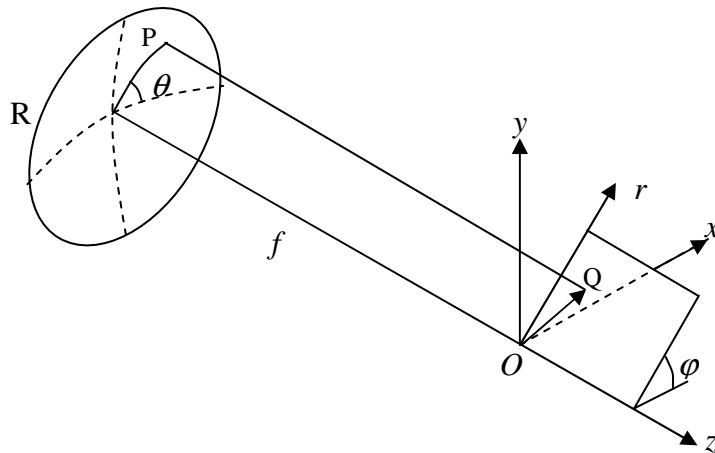


Fig. 1. Geometry and coordinates of the focusing problem.

The simplest design for the proposed trifocal lens is a base or carrier refractive (intraocular or contact) lens where one of the surfaces is cut into a diffractive profile. The shape of the diffractive surface is circularly symmetric with a radial cross-section of the form,

$$h(\rho) = h_0 \cos(2\pi a R^2 \rho^2), \quad (3)$$

where the h function represents the topographical height at any given point on the surface with respect to the base reference surface corresponding to the carrier refractive lens. The resultant optical height (optical path shift) due to the diffractive surface is,

$$h_{\text{opt}}(\rho) = (n_2 - n_1) h_0 \cos(2\pi a R^2 \rho^2) = b \cos(2\pi a R^2 \rho^2), \quad (4)$$

where n_1 and n_2 are the refractive indices of the lens material and the surrounding medium (lachrymal tear or intraocular fluid), respectively, and $b = (n_2 - n_1) h_0$.

If we assume a pure phase lens (absorption and reflections in the lens material are not considered), the complex pupil function of the multifocal lens can be written as,

$$P_{\text{lens}}(\rho) = \exp[i\Phi_{\text{lens}}(\rho)], \quad (5)$$

with the lens phase function Φ_{lens} being,

$$\Phi_{\text{lens}}(\rho) = k \left[b \cos(2\pi a R^2 \rho^2) - p_{\text{base}} (R^2 \rho^2 / 2) \right]. \quad (6)$$

In Eq. (6), the second term inside the bracket is the phase shift due to the base refractive lens that is assumed to contribute with p_{base} diopters to the optical power of the lens. The cosine term is responsible for the add diffractive optical powers. We can define the add diffractive power p_a as,

$$p_a = (f + \Delta f)^{-1} - (f)^{-1}, \quad (7)$$

Δf being the focal length shift due to the diffractive surface. The relation between the optical coordinate u and the add power is,

$$p_a = \frac{u}{R^2 + f u}. \quad (8)$$

We will see later that the parameter a governs the add diffractive power p_a (i. e. the distance between foci), and b controls the energy distribution among foci.

The analysis of performance of ophthalmic multifocal lenses in actual eyes can be done by including the eye pupil function in the PSF calculation. The eye pupil functions are obtained experimentally from ocular wave aberration functions measured with a Shack-Hartman wavefront sensor. The measurement provides the coefficients of an expansion of the phase aberration function in terms of the Zernike polynomials,

$$\Phi_{\text{eye}}(\rho, \theta) = k \sum_j c_j Z_j(\rho, \theta), \quad (9)$$

$Z_j(\rho, \theta)$ being the Zernike circular polynomials [15] and c_j the measured coefficients. The eye pupil function and the pupil function of the complete visual (eye + lens) system are,

$$P_{\text{eye}}(\rho, \theta) = \exp[i\Phi_{\text{eye}}(\rho, \theta)] \quad \text{and} \quad P(\rho, \theta) = P_{\text{lens}}(\rho) P_{\text{eye}}(\rho, \theta). \quad (10)$$

3. Trifocal lens design

In order to design trifocal lenses, we set up a realistic working context. We select a wavelength of $0.555 \mu\text{m}$, a pupil radius of 3.5 mm , and an eye focal length of 22.6 mm .

Figure 2 shows the calculated axial PSF of a lens with a phase profile following Eq. (6) with parameters $a = 1.724 \text{ mm}^{-2}$, $b = 0.127 \mu\text{m}$, and $p_{\text{base}}=0$. As we will see below, these parameters correspond to a trifocal lens of equal energy distribution among foci and 2D add power. The radial cross-section of the phase profile is shown in Fig. 3. The value of parameter b implies a peak to valley topographical height ($2h_0$) of $1.15 \mu\text{m}$ in the surface relief of the lens if we use 1.55 and 1.33 as the refractive indices of the lens material (PMMA) and surrounding medium (ocular fluid), respectively. The maximum phase shift between consecutive zones is 0.92π radians. It is worth noticing that most of the energy is contained into the three foci (90%) with only a 10% of the energy distributed along the axis out of the main foci. The usual diffractive bifocal lens only concentrates the 80% of the incoming light in the two foci, therefore the cosine design is more energy efficient.

A detailed inspection of Fig. 2 shows that the right focus is slightly displaced from -2D position. This happens because of the nonlinear dependence of the axial position in diopters with respect to the u coordinate (see Eq. (8)). When the axial direction is expressed in the optical coordinate u , the three foci are equally separated. The foci positions are given by $u_f = 0, \pm 2\lambda R^2 a$. By substitution in Eq. (8), the expected position is -1.8 diopters. The displacement can be translated to the left focus by modification of parameter a . If we set $a = 1.887 \text{ mm}^{-2}$, the right focus is at -2.0 diopters but the left one is at 2.2 diopters (the central focus is always at zero diopters). The shift increases for greater add powers.

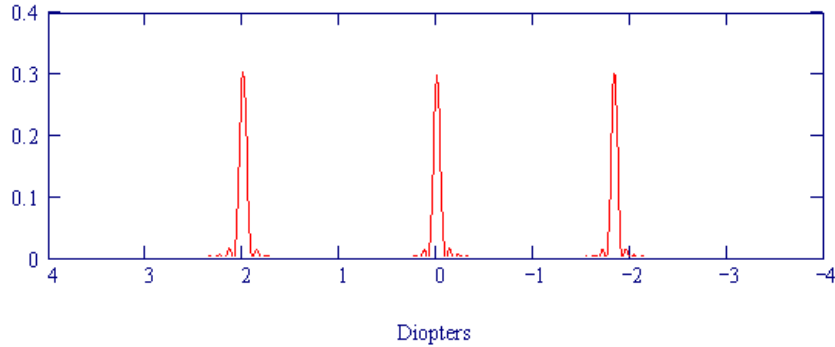


Fig. 2. Axial PSF of a trifocal lens with 2D add power ($p_{\text{base}} = 0$). The zero position corresponds to the eye focal point and the z axis is expressed in added diopters (Eq. (7)), so increasing z coordinate corresponds to decreasing add power. PSF normalization has been done by setting the PSF maximum of the eye without diffractive lens equals to one.

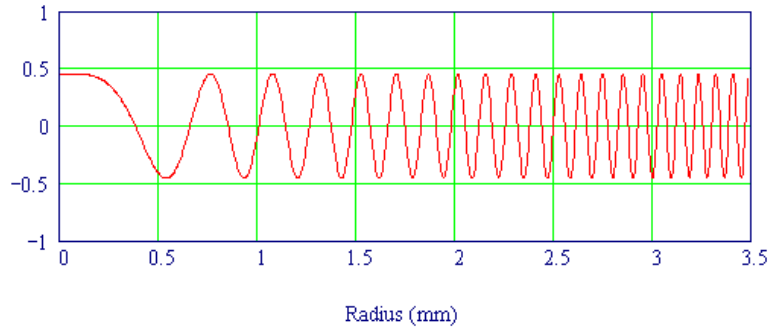


Fig. 3. Trifocal lens phase profile radial cross-section following Eq. 6 ($a = 1.724 \text{ mm}^2$, $b = 0.127 \mu\text{m}$, $p_{\text{base}} = 0$, and $R = 3.5 \text{ mm}$). Phase is in π units.

3.1. Eye pupil size effect

The eye pupil is size variable depending on the lighting conditions. Figure 4 shows the axial PSF of the previously described trifocal lens for three different pupil sizes 7, 5, and 3 mm. The foci positions and relative height do not change as the parameters a and b remain constant. However, the foci axial widths grow when the pupil size decreases. To maintain three separated foci, at least two periods of the cosine profile are needed. From Eq. (4), we obtain that the minimum pupil radius is $R_{\text{min}} = (2/a)^{1/2}$. In the case of the trifocal lens of 2D add power, the minimum pupil diameter allowed is around 2 mm, that is smaller than usual eye pupil diameter under photopic conditions.

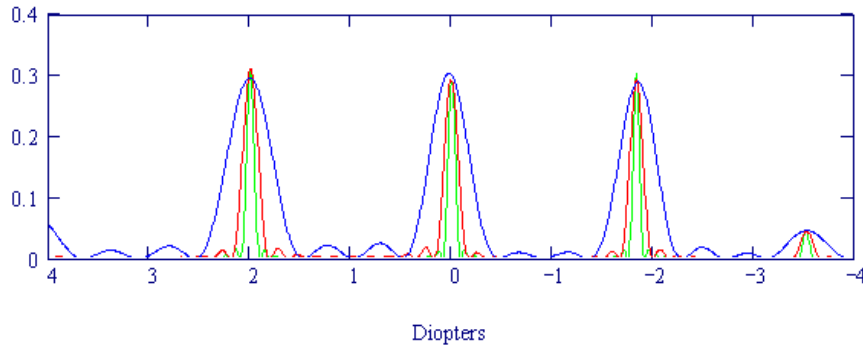


Fig. 4. Axial PSF of a trifocal lens (2D add power, $p_{\text{base}} = 0$) for three eye pupil diameters: 7 (green), 5 (red), and 3 (blue) mm. Each PSF is normalized with the corresponding PSF for the same pupil size without lens.

3.2. Transverse PSF

In order to verify the image forming quality of the lens, we have calculated the transverse PSFs on the three focal planes. The transverse PSF can be obtained from Eq. (1) by replacing the variable u with the focal plane positions $u_f = 0, \pm 2\lambda R^2 a$. For a circularly symmetric pupil function as the one described in Eqs. (5) and (6), the integration over θ also yields a circularly symmetric amplitude on the transversal planes $u = u_f$,

$$A(v, u_f) = A_0 \int_0^1 P_{\text{lens}}(\rho) J_0(k v \rho) \exp\left[-i k \frac{1}{2} u_f \rho^2\right] 2\rho d\rho, \quad (11)$$

where J_0 is the zero order Bessel function of the first kind. The transverse PSF is the squared modulus of Eq. (11). The three numerically calculated PSFs are almost identical to the Airy

PSF of the naked eye but with height 0.3. Hence, it is clear that all of them will produce the same image quality.

3.3. Foci distance control

As mentioned, the axial distance between foci is a function of the lens parameter a . It can be easily demonstrated that the positions of the foci are $u_f = 0, \pm 2\lambda R^2 a$. By substitution in Eq. (8), we found the relation between parameter a and add power p_a ,

$$a = \frac{P_a}{2\lambda(1 + f p_a)} \approx \frac{P_a}{2\lambda}. \quad (12)$$

Equation (12) provides the value of a needed for a desired add optical power. In Fig. 5 we show the axial PSF of a lens with add power 2D and $p_{base} = 2D$ ($a = 1.724 \text{ mm}^{-2}$, $b = 0.127 \mu\text{m}$, and $R = 3.5 \text{ mm}$). This lens achieves a range of focus of 4 diopters with clear vision at distances of infinity (with distant focus at $p_a = 0D$), 50 cm (with intermediate focus at $p_a = +2D$) and 25 cm (with near focus at $p_a = +4D$). This might be the case of an intraocular lens implanted to replace the crystalline lens.

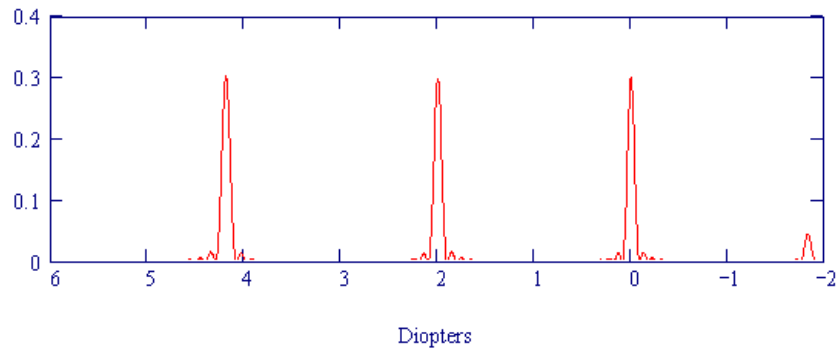


Fig. 5. Axial PSF of a trifocal lens with 2D add power and $p_{base} = 2D$ ($a = 1.724 \text{ mm}^{-2}$, $b = 0.127 \mu\text{m}$, $R=3.5 \text{ mm}$).

As a demonstration of the capability of the design parameter a , Fig. 6 shows, in a movie file, the axial PSFs of trifocal lenses with foci distance in the range 0.5 to 3 diopters (parameter a in the range 0.445 to 2.531 mm^{-2}). In all the cases the b parameter has been set equal to 0.127 μm corresponding to approximately equal height foci for each lens.

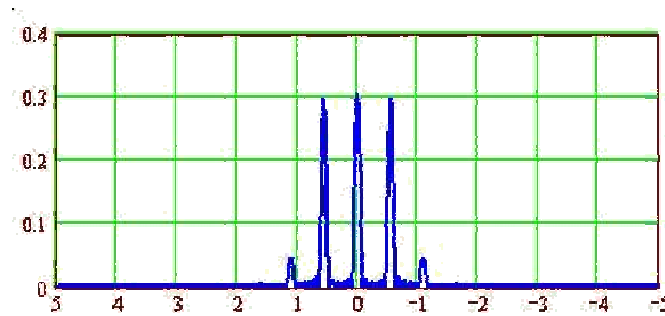


Fig. 6. Movie representation of axial PSFs of trifocal lenses with foci distance in the range 0.5 to 3 diopters (parameter a is in the range 0.445 to 2.531 mm^{-2} , $b = 0.127 \mu\text{m}$, and $R = 3.5 \text{ mm}$) (84KB).

3.4. Energy distribution control between foci

Light distribution control in multifocal lenses can be used to get better image contrast on a desired image plane. Bifocal intraocular lenses with asymmetrical light distribution in the distance and near focus to both eyes have been used in bilateral implantation to improve contrast visual acuity [10].

In the proposed trifocal lens, the energy distribution between foci (relative height of the axial PSF peaks) is governed by the design parameter b . It can be demonstrated that the heights of the peaks are $J_0(kb)^2$ and $J_1(kb)^2$ for the central and lateral peaks, respectively (J_1 is the first order Bessel function). The equal energy distribution corresponds to the condition $J_0(kb)^2 = J_1(kb)^2$, which yields to $b = 0.127 \mu\text{m}$, and peaks of 0.3 height. Figure 7 shows, in a movie file, the axial PSF of trifocal lenses ($a = 1.724 \text{ mm}^2$ and $R = 3.5 \text{ mm}$) with b in the range 0.103 to 0.149 μm , that is, from central focus double the height of the lateral foci to the reverse situation.

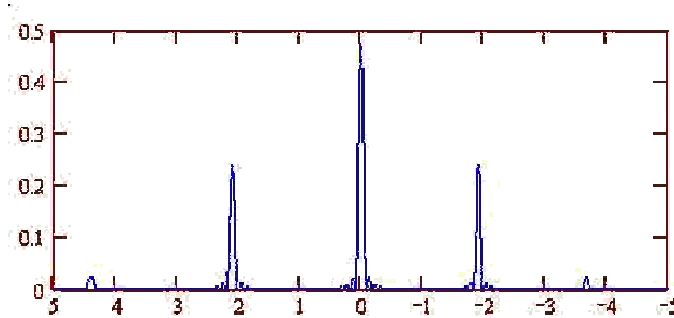


Fig. 7. Movie representation of axial PSFs of trifocal lenses with parameter b in the range 0.103 to 0.149 μm ($a = 1.724 \text{ mm}^2$ and $R = 3.5 \text{ mm}$), (24KB).

4. Effects of eye aberrations

Previous studies have shown that part of the subject's visual quality while wearing bifocal lenses can be predicted based on their aberrations. Particularly, it has been demonstrated that the lenses do not always provide bifocal vision but only an increase in depth of focus [16]. To investigate how the eye aberrations affect the optical performance of the trifocal lens, we have combined measured ocular wave aberrations with trifocal wave functions to obtain the axial and transverse PSFs of the whole visual system. We have used some previous experimental data obtained by Artal's group in a population of 84 healthy eyes using a Hartmann-Shack wave-front sensor [17]. The measurement provides the expansion coefficients of the aberration function in terms of the Zernike polynomials. These coefficients are introduced in Eq. (9) to obtain the eye pupil function.

To illustrate this procedure, we show in Fig. 8(a) the calculated axial PSF of an eye with a relevant amount of aberrations (its phase RMS is higher than the phase RMS of 2/3 of the 84 eyes). This axial PSF (blue line) deviates from the ideal aberration-free eye axial PSF (red line), in part because of the natural ametropias of this eye. The correction of the ametropias with eyeglasses or contact lenses can be simulated by changing the value of the corresponding Zernike coefficients. Figure 8(b) shows the axial PSF of the previous eye but correcting the primary astigmatism (the coefficients of Zernike polynomials $Z_{\pm 2}^2$ have been set to zero). The PSF is still about 0.75 diopters apart from the origin because of myopia.

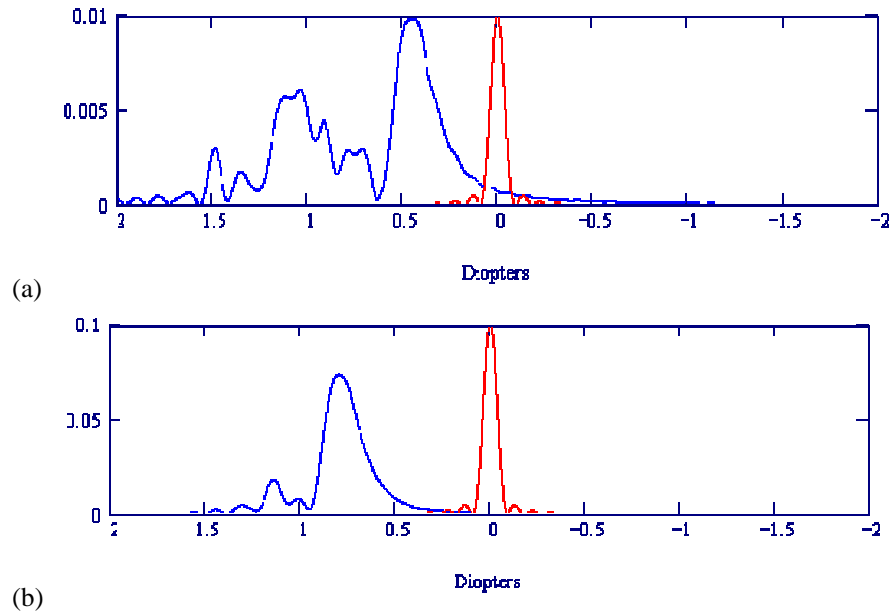


Fig. 8. (Blue line) Axial PSF calculated from measured aberration function of an actual eye. (a) uncorrected eye and (b) astigmatism corrected eye. For comparison, ideal aberration-free axial PSF is drawn with red line. (Pupil radius 3.5 mm and focal length 22.6 mm).

Since the transverse PSF of an actual (aberrated) eye may have a quite irregular shape, the intensity at the central point may not be a representative value of the axial behavior. A more adequate metrics to describe the through-focus variations is the Strehl ratio (defined as the maximum of the transverse PSF divided by the maximum of the diffraction-limited transverse PSF of the same pupil size [18, 19]). The axial variation of the Strehl ratio of the 2D add power trifocal lens in the corrected eye is shown in Fig. 9 ($a = 1.724 \text{ mm}^{-2}$, $b = 0.127 \mu\text{m}$, and $R = 3.5 \text{ mm}$). The base power p_{base} has been set to 1.25 diopters in order to both compensate the myopia (-0.75D) and locate the farsighted focus at the true focus of the eye (+2D). Basically, the Strehl ratio axial variation is repeated at the three foci of the lens and so the image forming capability will be very similar.

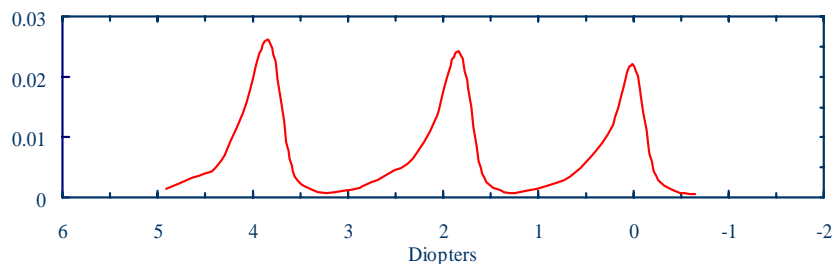


Fig. 9. Calculated Strehl ratio of the same eye as in Fig. 8(b) but while wearing a trifocal lens of 2D add power and $p_{base} = 1.25\text{D}$ ($a = 1.724 \text{ mm}^{-2}$, $b = 0.127 \mu\text{m}$, and $R = 3.5 \text{ mm}$).

It seems that the trifocal lens will provide distant, intermediate, and near clear vision. Nevertheless, when a distant object is viewed, a sharp retinal image is provided by the corresponding focus, and two somewhat blurred images are provided by the other two foci. The roles of the foci change when intermediate or near object are observed. In each situation,

the unwanted effect of the light in the out-of-focus images is to reduce the contrast of the infocus image [20].

To verify the image forming quality, we have also calculated the through-focus transverse PSF in Fig. 10 (movie file). On the right hand side, it shows the transverse PSFs of the eye along the axis passing through the three foci. For comparison, the PSF at the focal plane of the eye without lens is shown on the left hand side. On top of each image the axial coordinate u and the Strehl ratio are shown. As it can be seen, the transverse PSFs at the three foci (positions $u = -23.44, 0$, and 23.44) are similar to that of the naked eye but with some ring-like structure due to the other two foci.

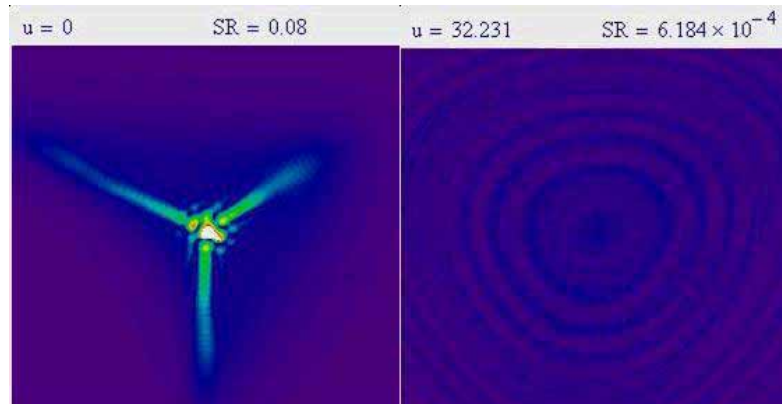


Fig. 10. Transverse PSF calculated from measured aberration function of an actual eye. (left) focal plane of the naked eye, (right) axial variation of the eye with a 2D add power trifocal diffractive lens. u is the axial coordinate and SR the Strehl ratio of each transverse PSF.

5. Multiple wavelength behavior

In the previous sections, we have considered multifocal diffractive lenses under monochromatic light conditions (at $\lambda=555$ nm, around the central wavelength of the photopic eye spectral sensitivity). The diffractive character of the lens makes the lens behavior wavelength dependent. For given values of the design parameters a and b , the distance and energy distribution of the foci change with wavelength. Different foci distance means longitudinal chromatic aberration. Figure 11 shows the axial PSF for the three wavelengths corresponding to approximately the peaks sensitivities of the three types of cones in the retina, 450 nm (blue), 540 nm (green), and 580 nm (yellow/red). The intermediate focus is at same position for all the wavelengths because it corresponds to the zero order diffraction that is not wavelength dependent. The lateral foci present about 0.5D aberration between blue and red but with opposite sign for near- and far-sighted focus. The nearsighted focus presents a chromatic aberration opposite to eye natural chromatic aberration. Natural aberration, between 450 nm and 580 nm, is about 1D [21], therefore it is partially compensated in the nearsighted focus case. As pointed out by other authors, the incorporation of a second diffractive surface may be useful to provide a degree of control over the chromatic aberration [1, 2].

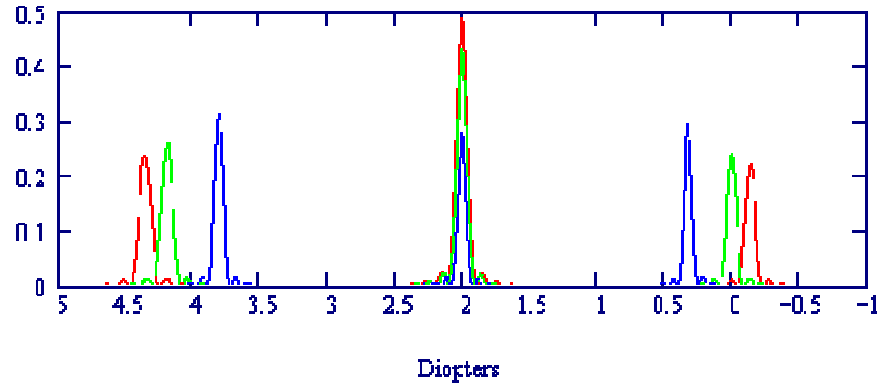


Fig. 11. Axial PSF of the same trifocal lens ($a = 1.724 \text{ mm}^2$, $h_0 = 0.104 \mu\text{m}$, $p_{\text{base}} = 2\text{D}$, and $R = 3.5 \text{ mm}$) for three different wavelengths, 450 nm (blue), 540 nm (green), and 580 nm (yellow/red).

6. Conclusions

We have used diffractive phase profiles able to split one beam into three beams to design trifocal lenses. It has been established the relationship between the parameters characterizing the phase profile (frequency and amplitude), and the lens optical features (add power or distance between foci and energy distribution). We have demonstrated that the add power and the light distribution among the foci are simple and independently controlled by two design parameters. We have also shown that the optical features do not depend on the variable eye pupil size. Uneven light distributions in the foci can also be achieved. The effects of eye natural aberrations on the lens performance have been simulated from measured ocular aberration data. To take full advantage of the multiple imaging property of trifocal lenses it is necessary for the eye to have a low level of aberrations, otherwise they must be compensated. The chromatic trifocal lens behavior has also been investigated.

A possible benefit of this study could be the design of ophthalmic multifocal lenses based on the patient's aberrations.

The calculus and simulation methods of this paper can be applied to the design and analysis of any other kind of diffractive or refractive multifocal contact or intraocular lens.

Acknowledgments

The authors are grateful to Artal's group at the "Universidad de Murcia" for the measured ocular wave aberration data. This research was supported by "Ministerio de Ciencia y Tecnología", Spain, grant BFM2003-03584.